# Metabolic impairments caused by a “chemical cocktail” of DDE and selenium in mice using direct infusion triple quadrupole time of flight and gas chromatography mass spectrometry

**Gema Rodríguez-Moro[1,2,3], Nieves Abril*[4], Rocío Jara-Biedma[1,2,3], Sara Ramírez-Acosta[1,2,3], José Luis Gómez-Ariza[1,2,3], Tamara García-Barrera*[1,2,3]**

*1. Department of Chemistry. Faculty of Experimental Sciences. University of Huelva, Huelva, Spain. 2. International Agrofood Campus of Excellence International ceiA3, University of Huelva, Huelva, Spain. 3. Research Center of Natural Resources, Health and the Environment (RENSMA). University of Huelva, Spain. 4. Department of Biochemistry and Molecular Biology, International Agrofood Campus of Excellence International ceiA3, University of Córdoba, Campus de Rabanales, Edificio Severo Ochoa, E-14071, Córdoba, Spain.*

Correspondence authors:
Prof. Tamara García-Barrera, Department of Chemistry, Faculty of Experimental Sciences, University of Huelva, Campus de El Carmen, 21007 Huelva, Spain
E-mail: tamara@dqcm.uhu.es
Phone: +34 959219962.

Dr. Nieves Abril, Department of Biochemistry and Molecular Biology, International Agrofood Campus of Excellence International ceiA3, University of Córdoba, Campus de Rabanales, Edificio Severo Ochoa, E-14071, Córdoba, Spain.
Phone: +34957218139.
E-mail: bb1abdim@uco.es

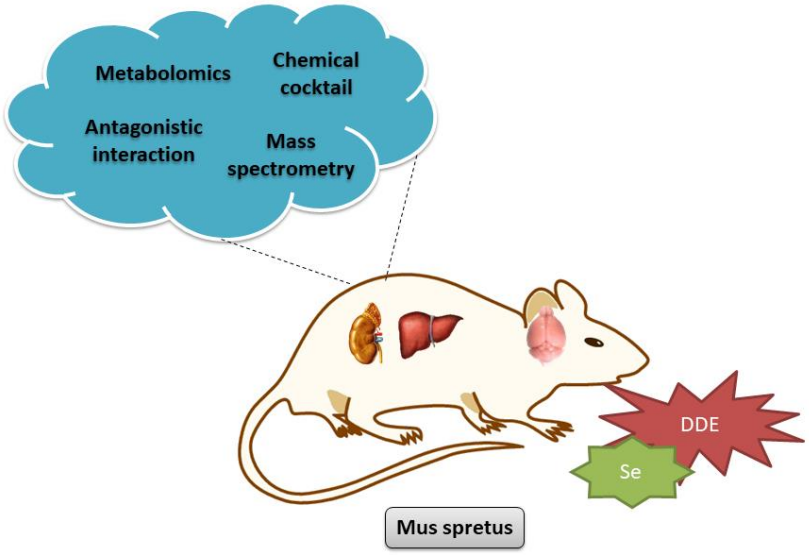


**Metabolic impairments in mice**

**Abstract**

Among the organic contaminants, pesticides are one of the most important groups of chemicals due to their persistent character and toxicity. However, the biological systems are exposed to a complex environment in which the contaminants can interact in a synergistic/antagonistic fashion and for this reason; the study of "chemical cocktails" is of great interest to fully understand the final biological effect. In this way, selenium is known for its antagonistic action against several toxicants. In this paper, the metabolic impairments caused by the joint exposure of *p,p´*-dichloro diphenyl trichloroethane (DDE) and selenium (Se) have been issued for the first time. A metabolomic workflow was applied to mice fed DDE and DDE with Se diet, on the basis of the complementary use of two organic mass spectrometric techniques, combining direct infusion mass spectrometry (DI-ESI-QqQ-TOF MS) and gas chromatography mass spectrometry (GC-MS). The results show a good classification between the studied groups caused by about 70 altered metabolites in liver, kidney or brain, including the pathways of energy metabolism, degradation of phospholipidic membrane, β-oxidation and oxidative stress, which confirm the potential of combined metabolomic platforms in environmental studies.

**Keywords:** DDE, pesticides, selenium, chemical cocktails, metabolomics, mass spectrometry

## 1. Introduction

The biological systems are exposed to a complex environment in which the contaminants can interact in a synergistic/antagonistic or agonistic fashion, and for this reason, the metabolism of toxic substances cannot be considered in isolation[1]. One of the most interesting elements is selenium that antagonizes mercury induced cardiovascular diseases[2], neurotoxicity[3], reproductive and developmental damages [4], arsenic-related skin lesions and cancer[5], cadmium-induced chromosomal aberrations[6] and general toxicity of metals forming insoluble complexes, eliminating free radicals[7] and many other toxic consequences of metal exposure. The protective effects of Se derive from its antioxidant properties, which intensifies the cellular antioxidant response against xenobiotics[8–10]. On the other hand, the chemical form of selenium is very important since several selenoproteins are peroxidases and oxidoreductases that protect against oxidative stress[9–12].

On the other hand, some reports demonstrated the Se protective action against the oxidative stress and lipid peroxidation caused by fenitrothion (organophosphate pesticide) in rats[13], as well as the benefits of Se combined with vitamin C on hemoglobin levels in farmers working with pesticide sprayers[14]. However, the combined biological response to Se and organic pollutants has not been extensively studied. Among the organic contaminants, one of the most persistent is 1,1,1-trichloro-2,2-bis(p-chlorophenyl)ethane (DDT) and its degradation product 1,1-Dichloro-2,2-bis(p-chlorophenyl)ethylene (DDE), classified as "likely to be carcinogenic to humans" by the Environmental Protection Agency (EPA). Toxicological data suggest that the liver is the

primary target organ of DDE toxicity in mammalian species[15]. DDE is an endocrine disrupter and antiandrogenic[16], as well as a known neurotoxic, implicated in Parkinson and Alzheimer disease[17] probably through the generation of oxidative stress[18]. DDE itself has no commercial uses and is only found in the environment as a result of contamination and/or breakdown of DDT[19](*EPA Report 815-R-08-012* 2008), but in some places it can be an abundant pollutant[20] because of its persistence and stability, causing its concentration and harmfulness rising along life[20]. The toxicity of DDE has been extensively studied, however the molecular mechanism underlying its toxicity remains unclear. Xenobiotics induce homeostatic imbalances producing compensatory mechanisms in cells and living systems that are finally reflected in gene expression changes at transcriptional level[21], the expression or inhibition of proteins as a consequence of traslational or post-traslational changes[22,23] and, in the final stage, very close to the phenotype, in the modification of metabolites implicated in the different cellular cycles (metabolomics)[24]. In a previous work[25], we demonstrated the ability of Se to modify the redox status and functionality of some proteins, and its role in maintaining cell homeostasis in the liver of DDE exposed mice.

Thus, to understand a cell, tissue or living organism behavior it is also necessary to consider low molecular mass molecules since they represent the last action mechanism of the organisms[26]. Organic mass spectrometry (MS) is frequently used in non-targeted metabolomics studies[27–29], either by direct introduction of sample extract in the spectrometer (direct infusion mass spectrometry-DIMS) or with a previous separation of extracts components (metabolites) by gas chromatography (GC) or high performance liquid chromatography (HPLC). The main advantages of HPLC-MS against DIMS are that the former can potentially resolve isomers, is less susceptible to ion suppression and in general, higher resolution of compounds that yield in-source fragments of lower molecular mass compounds in time[26]. DIMS has undoubted advantages in high throughput metabolomics analysis because it bypass the time-resolved introduction of metabolites into the mass spectrometer (MS) as consequence of chromatographic separation, increasing analysis rapidity and reproducibility, as well as metabolite coverage[30], any potential drawback caused by signal reduction associated to ion suppression is overcome with the use of diluted solutions[31]. For these reasons, DIMS is a good technique for a fast metabolomics approach with the aim of determining possible changes in important metabolic cycles caused by the action of organic and inorganic pollutants. However, the combination of direct infusion mass spectrometry and gas chromatography mass spectrometry (GC-MS) has been proposed for toxicometabolomic studies on living organisms[31], considering the complementarity of both techniques to extend the metabolic coverage and the availability of spectral libraries in GC-MS for metabolite identification[32].

In this work, the metabolic imbalances produced by the joint exposure to DDE and selenium have been studied for the first time in mammals using *Mus spretus* mice as model. The complex mechanisms that intertwine the transformation and excretion of DDE with selenium intake requiere the integration of complementary analytical platforms

for a metabolomic study, such as direct infusion electrospray quadrulole time of flight mass spectrometry (DI-ESI-QTOF-MS) and GC-MS, supplemented with statistic treatment of data (PLS-DA-partial least square discriminant analysis) to get deeper insight into the metabolism in this organism. The results of this work will help to explain our previous results in liver and proportionate a deep vision of the effect of DDE in kidney and brain.

## 2. Materials and methods

### 2.1. Animals, exposure protocol, reagents and samples

For the exposure experiments, *Mus spretus* mice of the consanguineous line SPRET/Ei were used to minimize the interindividual differences characteristic of free-living individuals. The animals were obtained from Jackson Laboratories (Bar Harbor, ME, USA). These mice were bred in the Centralized Animal Service of Experimentation of the UCO (SCAE-UCO), kept in a laboratory conditioned for them, with controlled photoperiod (12:12 h) and temperature (25 ± 2 °C), as well as water and laboratory diet *ad libitum*. Male mice of 7-9 weeks (11-13 g) were used. Mice were randomly divided into four groups (5 mice each, individually caged): (1) control group, (2) diet with a DDE dose of 150 mg/kg of chow, (3) diet with a sodium selenite dose of 4 mg/kg of chow and (4) diet combining those doses of DDE and sodium selenite. Selenium dose was selected taking into 3-fold the regular amount of Se in a rodent diet[25]. DDE dose was selected taking into account that mice liver lesions were identified at a Lowest-Observed-Adverse-Effects Level (LOAEL) by oral administration of 42.9 mg/kg bw/day[15,33] and our previous work [25]. On the other hand, the selected DDE dose is close to the mean Europe human population daily intake of DDE of 50 μg [34].

Food and water was replaced every second day and the consumed quantity recorded to estimate the daily ingest of Se and *p,p´*-DDE. After 30 days, mice were sacrificed by cervical dislocation, dissected using a ceramic scalpel and finally liver, kidneys and brain were rapidly transfer to dry ice. Individual organs were cleaned with 0.9% NaCl (w/w) solution, frozen in liquid nitrogen and stored at -80ºC until they were used for extract preparation.

All animals received humane care in compliance with the guidelines of animal care and use of the European Community and the experimental design was made seeking to minimize the number of animals and following the guidelines of the Bioethics Committee of the University of Córdoba (Spain). The protocol for this study was also reviewed and approved by the Regional Ministry of Agriculture, Livestock and Sustainable Development (Junta de Andalucía, Spain).

All reagents used for sample preparation were of the highest available purity. Sodium selenite and DDE were purchased from Sigma-Aldrich (Steinheim, Germany). Standards were dissolved in ultrapure water obtained with a System Milli-Q Direct 8/16 (Millipore, Watford, UK). The solvents used for metabolite extraction from tissues were of LC-MS grade. Methanol and acetonitrile were from Fisher Chemical (Geel, Belgium), while

ethanol, pyridine and formic acid were from Sigma-Aldrich (Steinheim, Germany). Formic acid was supplied by Merck (Darmstadt, Germany), and derivatizing agents for GC-MS analysis, namely, methoxylamine hydrochloride and N-methyl-N-(trimethylsilyl) trifluoroacetamide (MSTFA) were also obtained from Sigma Aldrich.

2.2. Sample preparation for metabolomic analysis

Metabolites extraction from individual tissues (liver, kidneys and brain) were carried out using a two-step procedure previously described[34] with several modifications. Organs were cryohomogenized using a cryogenic homogenizer SPEX SamplePrep (Freezer/Mills 6770) under liquid nitrogen during 30 s, at rate of ten strokes per second. After that, 30 mg of sample was mixed with 300 µL of extraction solvent containing MeOH with precooled 0.1% formic acid (for ESI-MS ionization in positive mode acquisition). The mixture was homogenized during 2 min using a pellet mixer (VWR, England, Uk) for cell disruption and then centrifuged at 12825 *g* for 10 min at 4ºC using a centrifuge model (Eppendorf AG, Hamburg, Germany). An aliquot of the supernatant (50 µL) was split for GC-MS analysis, and the remaining volume was transferred to the injection vial for DI-ESI-QqQ-TOF-MS analysis in positive and negative modes. Then, the pellet isolated during the first step was again extracted in order to recover the nonpolar fraction of metabolites. Thus, the precipitate was mixed with 300 µL of chloroform/methanol 2:1 (v/v) containing 10 mM acetate ammonium (for ESI-MS ionization in positive mode acquisition) and was homogenized and centrifuged as previously described. The supernatant was taken for the analysis by DI-ESI-QqQ-TOF-MS in positive and negative modes.

Derivatization for GC-MS analysis was carried out according to the two step methodology proposed by Begley et al with several modifications[35]. Briefly, 50 µL of the extract was dried under a nitrogen stream and redissolved in 50 µL of 20 mg/mL methoxyamine in pyridine for carbonyl groups protection by methoximation. After briefly vortexing, samples were incubated at 80°C for 15 min in a water bath. Then silylation was performed by adding 50 µL of MSTFA and incubating at 80°C for a further 15 min. Finally, extracts were centrifuged at 5130 *g* for 1 min and the supernatant was collected for analysis.

Furthermore, a total of seven Quality Control samples (QCs) were prepared by pooling equal volumes of all samples studied, which were treated with the described sample procedure and analyzed for GC-MS and ESI-QTOF-MS. In addition, a derivatization blank was used per batch of 6 sample extractions as the negative control. A reagent blank is testing for all chemicals detected in a GC-MS run that stem from impurities or contaminations that were included in tubing, glass, plastic ware, or the reagents themselves.

**2.3. Metabolomic analysis**

Gas chromatographic analysis was performed in a Trace GC ULTRA gas chromatograph coupled to an ion trap mass spectrometer detector ITQ900 (Thermo Fisher Scientific),

using a Factor Four capillary column VF-5MS 30 m × 0.25 mm ID, with 0.25 μm of film thickness (Varian). The GC column temperature was set to 100 °C for 0.5 min and programmed to reach 320 °C at a rate of 15 °C per minute. Finally, this temperature was maintained for other 7 min, being the total time of analysis 22.17min. The injector temperature was kept at 280 °C, and helium was used as carrier gas at a constant flow rate of 1ml $min^{-1}$. For mass spectrometry detection, ionization was carried out by electronic impact (EI) with a voltage of 70 eV, by full scan mode in them/z range 35–650, with anion source temperature of 200 °C.

The DI-ESI-QTOF-MS experiments were performed in a QSTAR XL Hybrid system (Applied Biosystems, Foster City, CA, USA) using the electrospray (ESI) source. The samples were introduced into the mass spectrometer at 5 μl/min flow rate using an integrated apparatus pump and a 1000 μl volume Hamilton syringe. Data were obtained in both positive and negative ionization modes, acquiring full scan spectra for 0.2 min in the m/z range 50–1100 uma with 1.005 s of scan time. MCA-multichannel averaging acquisition was 10 in all the cases. The parameters of the Q-TOF system were optimized to obtain the a higher sensitivity with minimal fragmentation of molecular ions. In positive mode, the ion spray voltage (IS) was set at 3300 V, and high-purity nitrogen was used as a curtain and nebulizer gas at flow rates about 1.13 l/min and 1.56 l/min, respectively. The source temperature was fixed at 60 °C, with a declustering potential (DP) of 60 V and a focusing potential (FP) of 250 V. The ion energy (IE) was fixed at 2.0 V with a channel electronmultiplier (CEM) of 2150 V. To acquire MS/MS spectra, nitrogen was used as collision gas.

### 2.4. Data processing and statistical analysis

Raw data were processed following the method described by Katajamaa and Oresic[36] which proceeds through multiple stages including feature detection, alignment of peaks and normalization. To this end, the freely available XCMS software, included in the R platform (http://www.r-project.org) was used. Files were converted into net CDF using the Thermo File Converter tool (Thermo Fisher Scientific) and subsequently, data were extracted using the matched filter method. This algorithm slices data into extracted ion chromatograms (XIC) on a fixed step size, and then each slice is filtered with matched filtration using a second-derivative Gaussian as the model peak shape[37]. The XCMS parameters were optimized according to the characteristics of datasets obtained in order to extract the maximum information as possible. Finally, the settings applied for GC-MS data were S/N threshold 2, full width at half-maximum (fwhm) 3, and width of the m/z range 0.1 (step parameter). After peak extraction, grouping and retention time correction of peaks (alignment) was accomplished in three iterative cycles with descending bandwidth (bw) from 5 to 1 s. For data normalization, the locally weighted scatter plot smoothing (LOESS) normalization method was used, which adjusts the local median of log fold changes of peak intensities between samples in the data set to be approximately zero across the whole peak intensity range[38]. The preprocessed data were then exported as a .csv file for further data analysis by multivariate procedures.

GC-MS data was processed with SIMCA-P™ software (version 11.5, published by UMetrics AB, Umeå, Sweden) to perform partial least squares discriminant analysis (PLS-DA) in order to discriminate between the groups of the study. Performance of models was assessed by the $R^2$ and $Q^2$ values, provided by the software (indicative of class separation and predictive power of the model, respectively). Finally, metabolites responsible for discrimination were selected according to the Variable Importance in the Projection, or VIP (a weighted sum of squares of the PLS weight, which indicates the importance of the variable in the model), considering only variables with VIP values higher than 1, indicative of significant differences among groups. NIST Mass Spectral Library (version 08) was used to identify the altered metabolites, considering only those variables with a probability greater than 80% as well as Kovats´retention indices of the compounds. Later, metabolites were identified using fragmentation analysis by MS/MS and matching the resulting fragmentation spectra with different DIMS-based metabolomics databases, such as Human Metabolome Database (http://www.hmdb.ca), METLIN (http://metlin. scripps.edu) and Mass Bank (http://www.massbank.jp). According to recommendations by the Metabolomics Standards Initiative (MSI)[39,40], the metabolites are identified to MSI Level 2.

For metabolomic data from DI-ESI-QTOF-MS analysis, Markerview™ software (Applied Biosystems) was used to filter the mass spectrometry results and to carry out the reduction into a two-dimensional data matrix of spectral peaks and their intensities. For this purpose, a filter intensity of 10 counts was used to eliminate non-significant variables from the dataset. Finally, data were normalized according to the total area sum to correct possible instrumental drifts. Before statistical analysis, data was submitted to Pareto scaling, for reducing the relative importance of larger values, and logarithmic transformation, in order to approximate to a normal distribution[41]. Then, data were subjected to statistical data analysis (partial least squares discriminant analysis, PLS-DA) by the SIMCA-P™ software package as above described for GC-MS data analysis.

Statistical significance was determined by using one-way ANOVA validated by Levene´s test, testing the homogeneity of variance and trusting only *p*-values with *p* Levene lower than 0.05. When statistical differences appeared by using ANOVA for any of the comparisons, differences about the means were compared using Tukey´s test (STATISTICA 8.0 sotfware, StatSoft, Tulsa, USA), using a level of probability of 0.05 as criterion for significance.

## 3. Results and discussion

To evaluate their effects and putative interactions on the liver, kidney and brain of *Mus spretus* mice, Se and p,p´-DDE were added to their diet for one month. During the treatment, the animals did not show perceptible signs of distress, disease or behavior disorders. No significant differences were observed in the food/water daily ingest neither All experimental groups ingested similar food/water intake was similar among groups, resulting in a daily ingest of approximately 0.32 mg/kg bw of Se and 37.5 mg/kg bw of DDE. The mice body weight was measured at the beginning and end of the experiment,

and no differences were observed between the control and treated groups. The t-test was applied to determine that no statistically significant differences were caused by the treatments. After sacrifice, no significant differences were found in bw or the appearance and weight of the different internal organs.

### 3.1. Metabolomic study of mice liver, kidneys and brain by combined analysis using DI-ESI-QTOF-MS and GC-MS

As described above, polar and nonpolar metabolites from liver, kidney and brain of mice exposed to selenite or/and DDE were obtained and analyzed by DIMS using ESI as ionization source (in positive -ESI$^+$ and negative -ESI$^-$ modes). The results obtained using negative mode of acquisition for nonpolar extracts had poor discrimination between different exposure groups. Figure 1 and 2 show the typical mass spectra of polar and nonpolar extracts, respectively obtained from mice livers of the different studied groups, after 30 days of the experiment analyzed by DI-ESI(+)QTOF-MS.

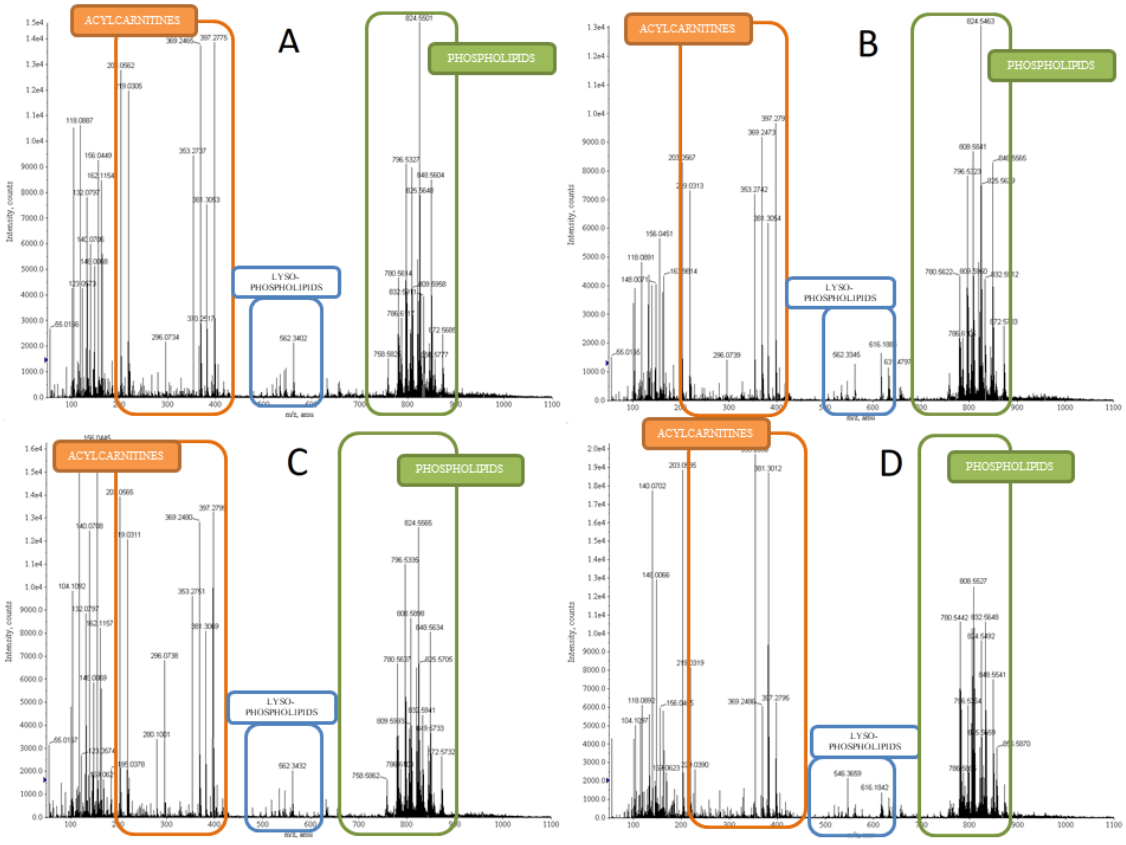


**Figure 1.** Typical DI-ESI(+)QTOF-MS spectra of liver polar extracts. A) Control group, B) diet with DDE (37.5 mg/kg bw/day), C) diet with selenite (0.320 mg/kg bw/day) and D) diet with DDE (37.5 mg/kg bw/day) and selenite (0.320 mg/kg bw/day).

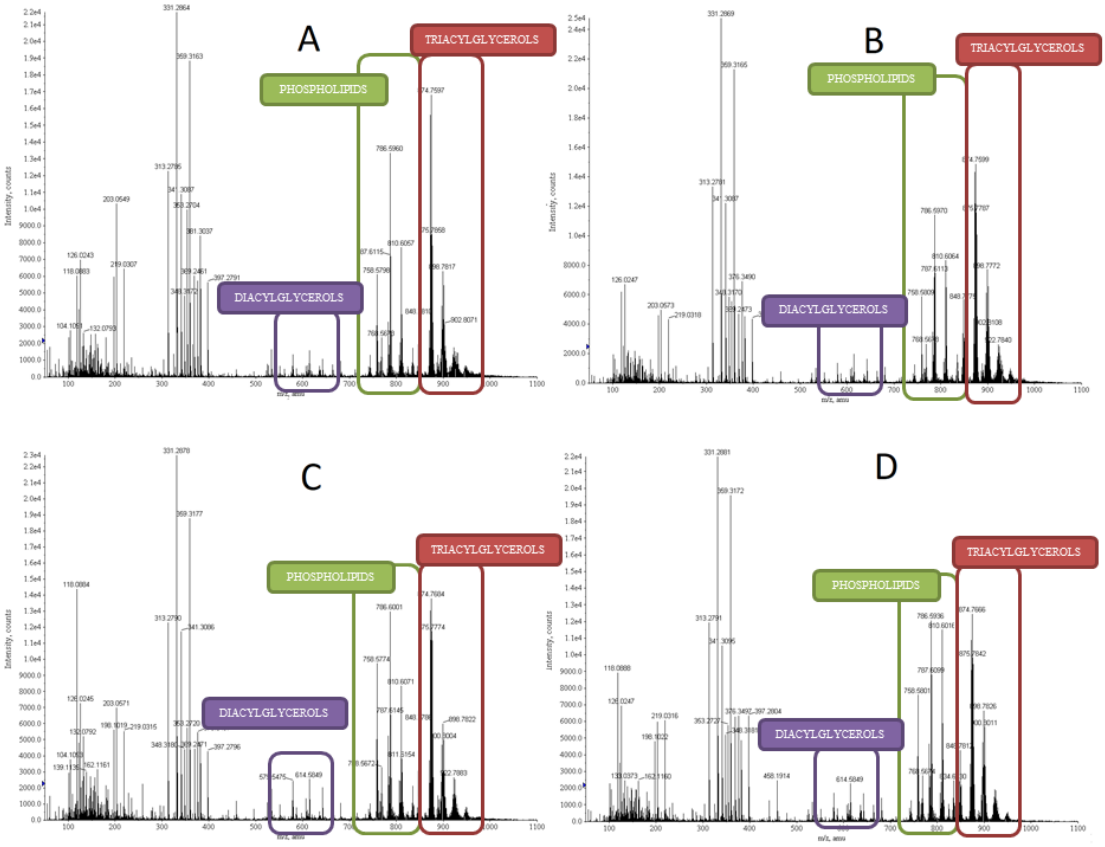


**Figure 2.** Typical DI-ESI(+)QTOF-MS spectra of liver nonpolar extracts. A) Control group, B) diet with DDE (37.5 mg/kg bw/day), C) diet with selenite (0.320 mg/kg bw/day) and D) diet with DDE (37.5 mg/kg bw/day) and selenite (0.320 mg/kg bw/day).

The hepatic polar extract spectra obtained by ESI(+)-QqQ-TOF-MS (Figure 1) provides a broad metabolomic profile, with signals in a range of *m/z* between 50-1000. Most of these signals are found at low *m/z* values (50-400) with different intensities, but above *m/z* 400 different clusters can be found, in which structurally analogous compounds, such as lysophosphatidylcholines, are probably concentrated (LPCs, *m/z* 500-600). Spectra of hepatic nonpolar extracts (Figure 2) were very similar to that obtained for the polar extracts. However, there are notable differences in the intensities of the signals, since the intensity of the clusters obtained from *m/z* 500 is increased in the apolar extract (indicating that they are probably lipid compounds), while for the lower part of the spectrum a decrease in sensitivity is observed in some signals. In addition, new clusters of peaks appear in the region of 650-750 *m/z* and 850-950 *m/z*, related to diacylglycerides and triacylglycerides. The addition of ammonium to the apolar extracts before acquisition causes the formation of adducts [M-$NH_4^+$] of these families of compounds since $NH_4^+$ enhances the ionization and detection.

Supplementary material shows the typical spectra obtained by ESI-QTOF-MS analysis for kidney (polar and nonpolar, Figures S1 and S2, respectively) and brain (polar and nonpolar, Figures S3 and S4, respectively). Kidney polar extracts (Figure S1 in the Supporting Information) present high intensity peaks in the range of 300-400 m/z, which correspond to acylcarnitines. In addition, a cluster of peaks in the m/z range 700-850 that

matches with phospholipids can also be observed. On the other hand, nonpolar extracts obtained from this organ (Figure S2 in the Supporting Information) shows a high intensity cluster of peaks in the range 800-950 m/z due to the presence of tryacylglycerides. The mass spectra obtained from polar and nonpolar extracts of brain (Figures S3 and S4 in the Supporting Information, respectively) are very poor. Even so, peaks corresponding to phospholipids can be observed in the range 700-850 m/z in both extracts.

The intensities of the *m/z* signals from liver polar and nonpolar extracts obtained by ESI-QTOF-MS and GC-MS were used to construct the PLS-DA models. Firstly, the score plots corresponding to the Principal Components Analysis (PCA) of the results of *Mus spretus* exposed to DDE with and without Se show clusters of samples with no abnormal value or outliers.

The scores plots corresponding to the PCA also showed a good grouping of the Quality Control samples (QCs), indicating low variability in the measurement and therefore a good reproducibility of the analytical method used. The results obtained using negative mode in polar and nonpolar extracts of liver showed low discrimination between the different exposure groups (results not shown). However, score PLS-DA plots from polar and nonpolar extracts in positive ionization mode give a good classification between the different study groups based on DDE and Se exposure (Figure 3). In turn, the values of the quality parameters of the $R^2$ and $Q^2$ methods confirmed a good discrimination of the different exposure groups ($R^2 = 0.98$ $Q^2 = 0.66$ for GC-MS, $R^2 = 0.99$ $Q^2 = 0.65$ for DI-ESI-QTOF-MS/nonpolar extract, $R^2 = 0.98$ $Q^2 = 0.76$ for DI-ESI-QTOF-MS/polar extract).

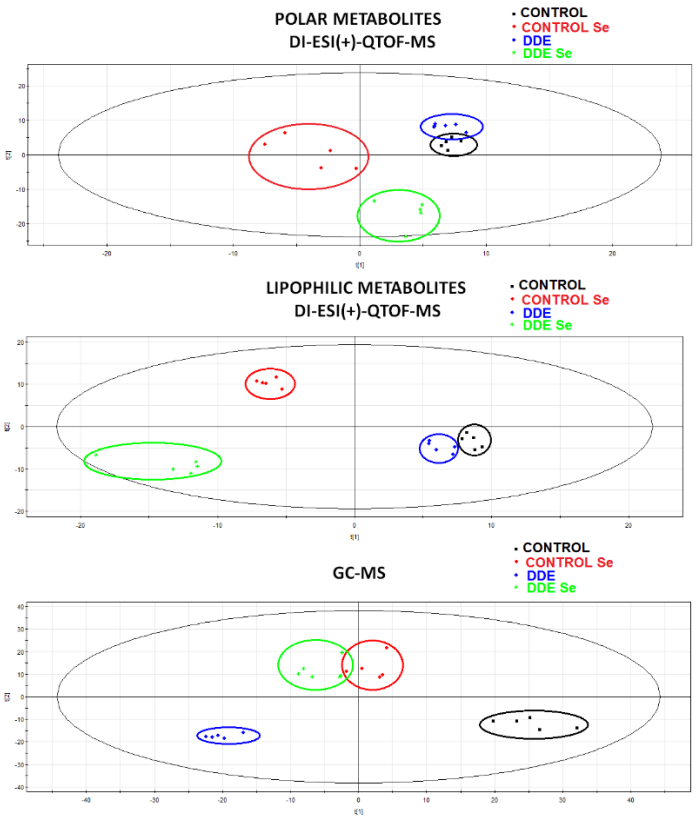


**Figure 3.** Scores Plots obtained by partial least square discriminant analysis of polar and nonpolar liver extracts of *Mus spretus* mice by ESI(+)-QTOF-MS and GC-MS. Circles have been drawn to show grouping of samples and they have not been obtained by statistical methods. The scores plots obtained for kidney and brain are shown in the supplementary material (Figures S5 and S6 in the Supporting Information, respectively).

From these plots can be inferred that Se interact with DDE causing metabolic alterations that are different, at least in part, to those caused by DDE alone. As discussed in our previous work [25], at the proteomic level, Se selectively acts on specific protein target, remodeling its functionality, but it is not able to completely prevent some of the cell alterations caused by DDE exposure, which could result even exacerbated. In fact, data indicate that the presence of Se could aggravate part of the DDE effects.

From the PLS-DA analysis, in which the different groups are clearly separated, the m/z ions used as variables which are driving the separation were further identified after MS/MS and database analysis (Tables 1 and 2).

PLS-DA analysis was also carried out in the kidney and brain metabolomic data obtaining similar conclusions (supplementary material). The scores plots (Figures S5 and S6) show a clear separation between the studied groups for the different acquisition modes in DIMS-QqQ-TOF-MS and GC-MS analysis, indicating the presence of differentially expressed metabolites in *Mus spretus* mice fed DDE and/or selenite diet.

### 3.2. Identification of altered metabolites in liver, kidney and brain of *Mus spretus* mice fed DDE and/or selenite diet.

To identify which variables were responsible for the above described separation in PLS-DA, the variable influence on the projection (VIP) was used. Only the variables with VIP>1 were selected to identify altered metabolites after DDE and/or selenite addition in food, which were identified by MS/MS experiments and open access metabolomic databases (HMDB, METLIN and Mass Bank). Tables 1 and 2 show a summary of the metabolites identified using both analytical techniques (ESI-QTOF-MS and GC-MS) in liver, kidneys and brain of mice fed with DDE, DDE with selenium and selenium diet as well as the relative response and fold change against the control group. As can be seen, complementary results are obtained using both techniques. The accession numbers of the metabolites are collected in the supplementary material (Table S1 in the Supporting Information). Table S2 and S3 in the Supporting Information shows summary stats on the RSDs/ CVs of the metabolites, samples run and number of identified metabolites.

The loadings plots (data not shown) allows obtaining the metabolite distribution against principal components (PC1 and 2), as well as the relative weight of each metabolite in the classification of the experimental studied groups (VIP) and the final response of the metabolite against the control group (down- and up-regulated). The identification of the lipids with ESI-QTOF-MS by tandem mass spectrometry was performed based on their characteristic fragmentation patterns. *Choline* containing phospholipids were detected as protonated ions and sodium adducts. Specifically, *lysophosphatidylcholines* (LPCs) presented characteristic ions at 184, 104 and 86 *m/z* and two typical fragments due to the loss of trimethylamine (*m/z* 59) and phosphocholine (*m/z* 183). On the contrary, in the case of the *lysophosphatidylethanolamines*, the product ion $[M + H\text{-}141]^+$ corresponding to the loss of the ethanolamine group was observed. The *diacylglycerols* (DAG) and *triacylglycerols* (TAG) were only detected by ESI (+)-QqQ-TOF-MS analysis of the nonpolar extracts. The fragmentation DAG and TAG occurs through the release of fatty acids that generate different types of ions (called A, B, C and D), which show characteristic values of *m/z* depending on the fatty acid attached to the main chain of glycerol[42]. Finally, *acylcarnitines* (CAR) were identified based on their characteristic fragments of 60.08 *m/z* for $[C_3H_9N + H]^+$ and 85.03 *m/z* for $[C_4H_5O_2]^+$ [43].

Figures 1 and 2 show the typical mass spectra obtained from livers of mice in the different exposure groups, that were later identified and discussed in the following sections. Differences were found among the different exposed groups as in the case of metabolites at *m/z* 750-950 in the nonpolar extract, which have been identified as triglycerides. In this *m/z* range, figure 2 shows a decrease in the DDE against the control group. Moreover, this effect is modulated in the mice fed DDE and Se diet. On the other hand, *lysophospholipids* (LPLs) resulted to be good biomarkers for the groups under study and in this sense, figures 1 and 2 show a decrease in LPLs (*m/z* 490-600) in the exposed groups against to the control and into a lesser extent against mice fed Se diet. The decrease of LPLs has been previously used as a biomarker in mice exposed to others toxic metals, as

Hg[44] and As/Cd[45]. At the same time, an increase in fatty acids (*m/z* 200-400) was observed in the groups exposed to DDE, which together with the decrease of LPLs can be related to the degradation of the phospholipidic membrane (cell apoptosis), as discussed in section 3.3[44].

The identification of metabolites by GC-MS, was carried out by retention time matching with standards (when available at our laboratory) and by comparing the mass spectra (full scan mode) with those of the NIST database (NIST 2.0). In general, the results obtained by ESI-(+)-QTOF-MS show changes in different classes of lipids including phospholipids, lysophospholipids, acylcarnitines, fatty acids and also low molecular weight metabolites. Alternatively, the results obtained by GC-MS show alterations in numerous primary metabolites (low molecular mass metabolites) such as amino acids, nucleotides, organic acids or carbohydrates.

### 3.2.1. Traffic of metabolites between organs

As it is well known, the most metabolically active organs are liver and kidneys. Most compounds absorbed by the intestine first pass through the liver, which is thus able to regulate the level of many metabolites in the blood and it also plays a central role in the homeostasis of lipids, carbohydrates and proteins metabolism[46]. Liver is also the sole organ able for *de novo* synthesis of fatty acids by lipogenesis and it is the main site for fatty acids oxidation together with the muscle[47]. However, fatty acids, which are one of the most important group of altered metabolites, as discussed in the next paragraphs, do not serve as fuel for the brain, because they are bound to albumin in plasma and so do not traverse the blood-brain barrier[28]. On the other hand, the major purpose of the kidney is to produce urine, which acts as a vehicle for excreting metabolic waste products and for maintaining the osmolarity of the body fluids.

Table 1 shows that DI-ESI-QQQ-TOF allows identifying 16 metabolites which were altered in liver, 17 in kidneys and 17 in the brain of mice under study. Five of them were altered in kidney and liver, four in kidney and brain and two in liver and brain. On the other hand, Table 2 shows that using GC-MS, 20 metabolites were detected to be altered in the liver of mice under study, 23 in kidneys and 13 in brain. Six of them were altered in kidney and liver, ten in kidney and brain and three in all the organs.

Several metabolites present different response in the different organs under study indicating a possible traffic between organs. Comparing liver and kidney, five metabolites altered present the opposite tendency between these organs. This is the case of *DAG (18:2/18:1)* and *ornithine* in mice fed DDE diet and *TAG (18:4/18:4/20:4)*, *TAG (16:0/18:1/22:0)* and *TAG (18:4/18:4/22:6)* in mice fed DDE, DDE with Se and Se diet. Moreover, all the metabolites altered in brain and liver (*choline* and *C18:1-CAR*), present the opposite response between these organs in mice fed DDE diet (Table 1). Finally, only two metabolites present the opposite response between kidney and brain, namely *betaine* in mice fed DDE diet and (iso-)*citrate* in mice fed DDE and DDE with Se diet. As above

commented, there are three metabolites altered in liver, brain and kidney, namely, *aspartic*, *uric* and *oleic acid*, which in turn present different response between them.

### 3.2.2. Antagonism between Se and DDE

It is important to compare the responses of mice fed DDE, DDE+Se and selenium diet against the control group to deep insight into the protective effect of selenium against the toxic effect of DDE. Figure 4 shows the fold changes of metabolites altered in the group of DDE which response is inverted after DDE+Se. As can be observed in Table 1, selenium counteract the effect of DDE on seven metabolites because they show a different response among the studied groups when they are compared against the control, namely: (i) *betaine*, which increases in the kidney of mice fed DDE diet (1.26-fold), while decreases in mice fed DDE+Se diet (0.78-fold) or Se (0.54-fold), (ii) *glutamate*, which increases in the brain of mice fed DDE diet (1.15-fold), while decreases in mice fed DDE+Se diet (0.49-fold), (iii) (iso-)*citrate*, which increases in the kidney of mice fed DDE diet (0.37-fold), while decreases in mice fed DDE+Se diet (0.52-fold) and Se diet (0.43-fold), (iv) *inosine*, which decreases in the kidney of mice fed DDE diet (0.61-fold) and DDE+Se diet (0.84-fold), while increases in mice fed Se diet (1.22-fold), (v) *DAG (18:3/18:1)*, which decreases in the kidney of mice fed DDE diet, while increases in mice fed DDE+Se and Se diet and (vi) *DAG (18:2/18:1)*, which decreases in the kidney of mice fed DDE diet (0.58-fold), while increases in mice fed DDE+Se diet (1.61-fold) and Se (2.70-fold), and (vii) *LPC (18:1)*, which decreases in the liver of mice fed DDE diet (0.47-fold), while increases in mice fed DDE+Se diet (0.78-fold) and Se diet (0.72-fold).

Table 2 shows that using GC-MS, only three metabolites present were different in the group of mice fed DDE or DDE with selenium diet against the control, namely: (i) *urea*, which increases in the kidney of mice fed DDE diet (1.62-fold), while decreases in mice fed DDE+Se diet (0.39-fold), (ii) *glutamine*, which increases in the kidney and brain of mice fed DDE diet (2.92- and 1.29-fold, respectively), while decreases in mice fed DDE+Se diet (0.19- and 0.24-fold, respectively) and (iii) *phosphoric acid*, which increases in the kidney of mice fed DDE diet (2.36-fold), while decreases in mice fed DDE+Se diet (0.48-fold) and Se diet (0.47-fold).
It is also remarkable that these antagonistic interactions between DDE and Se usually take place in kidney, since the majority of metabolites that present different response between the mice fed DDE and DDE with Se diet occur in this organ.

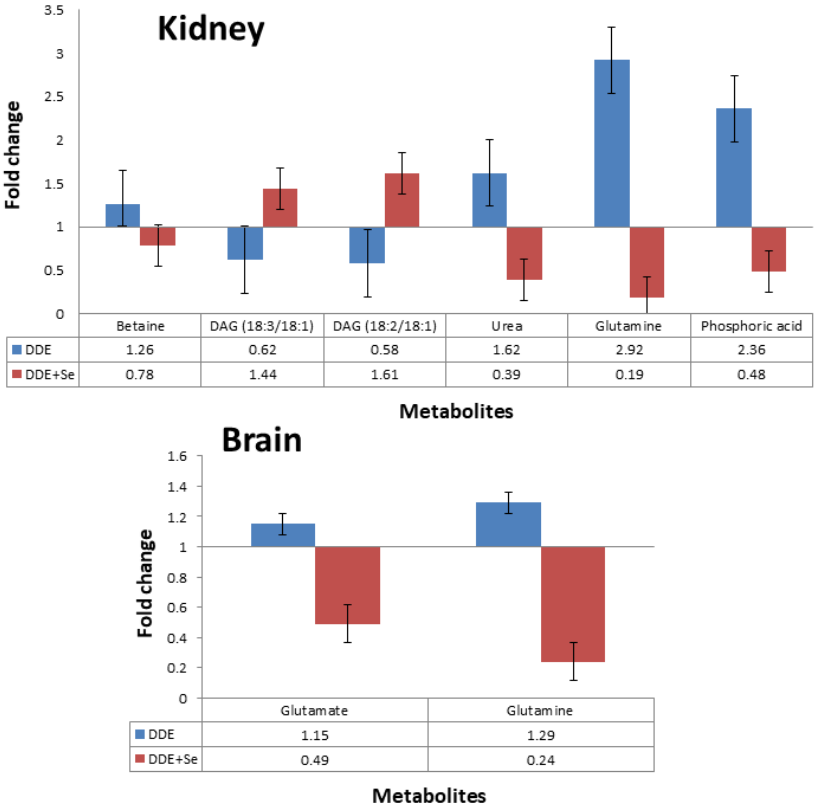


**Figure 4.** Bar graphs representing the fold changes of metabolites altered in the group of DDE which response is inverted after DDE+Se.

### 3.3 Biological interpretation

Tables 1 and 2 show the metabolites altered in mice fed DDE and Se diet indicating the pathway and other metabolomic studies in which it was detected. On the other hand, Figure 5 summarizes the number of metabolites that have been found to be significant in each organ and exposure group under study after GC-MS and QTOF analysis.

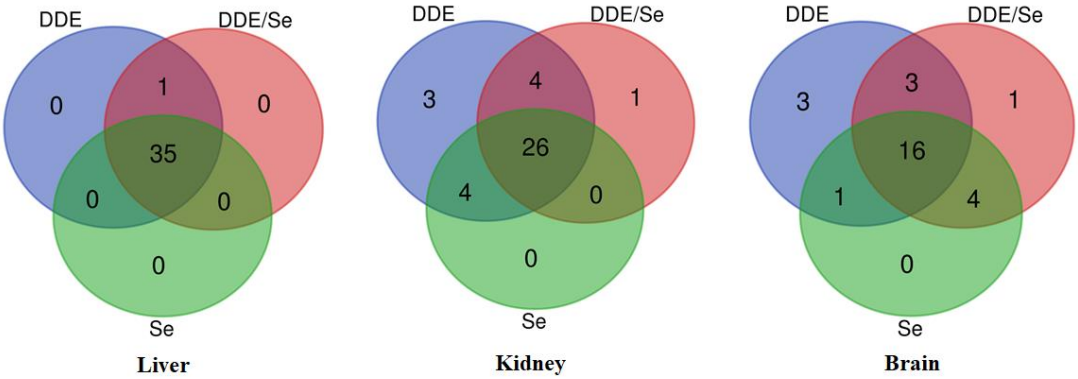


**Figure 5.** Venn diagram showing the number of significant metabolites identified in each exposure group against the control in liver, kidney and brain. Exposure groups: Se, DDE (mice fed DDE diet) and DDE/Se (mice fed DDE and selenium diet).

Pathway analysis was conducted using the Metaboanalyst 4.0 web tool (https://www.metaboanalyst.ca/) to decipher the most important pathways altered after the exposure of DDE. The "*Mus musculus*" library was selected using the default "Hypergeometric Test" and "Relative-Betweenness Centrality" algorithms for pathway enrichment analysis and pathway topological analysis, respectively. In order to identify the most relevant pathways, the impact-value threshold calculated from pathway topology analysis was set at 0.1. Figure 6 shows the main altered pathways after DDE exposure in liver, brain and kidney. The most altered pathways are: linoleic acid, glycerolipid metabolism and alanine, aspartate, and glutamate metabolism in liver; linoleic acid metabolism and glycine, serine and threonine metabolism and methane metabolism in kidney; and finally glutamine and glutamate metabolism and alanine, aspartate and glutamate metabolism in brain. P-values and pathway impact scores for the most significant pathways of each organ are provided in the Table S4 in the Supporting Information. These pathways are discussed in the following sections.

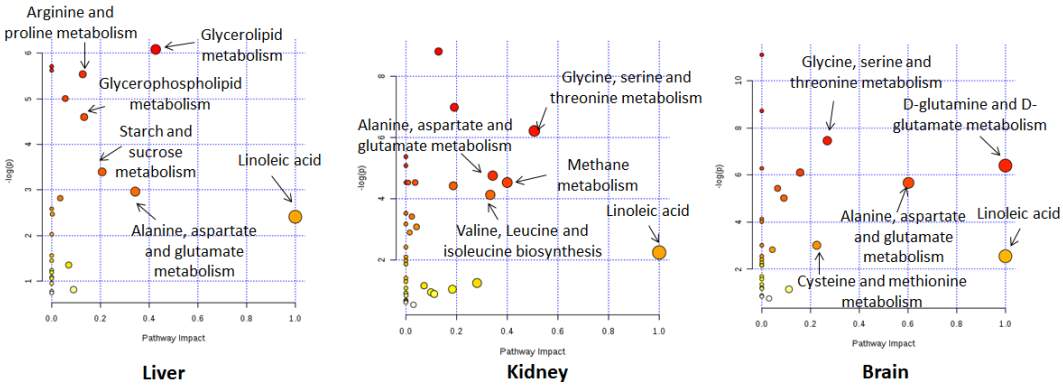


**Figure 6.** Summary chart of the interconnected metabolic pathways related to altered metabolites in liver, kidney and brain after DDE exposure.

### 3.3.1. Arginine and proline metabolism.

The influence of DDE exposure on this pathway is supported by the increase of *proline* in all the studied groups in kidney and brain (Tables 1 and 2) and the decrease of creatinine in liver. Proline protects during stress by serving as a direct scavenger of reactive oxygen species and also by helping maintain cellular energy and NADP+/NADPH balance[48]. However, increased concentrations of proline induce oxidative damage. Nitrogen recycling from arginine to glutamate in the ornithine pathway appears to be the cause of stress-induced proline accumulation[48]. Arginine is also a precursor of creatine, involved in the creatine-phosphocreatine system for energy transport. Creatinine is mostly formed from phosphocreatine in muscle and brain. In mammals, creatine is phosphorylated to phosphocreatine by creatine kinase (CK), and oxidative stress favors the nonenzymatic conversion of creatine through the reaction of the carboxyl and amino group of phosphocreatine[49,50]. CK is very susceptible to oxidative stress due to the presence of a highly reactive sulfhydryl group (Cys-283) that causes the

inhibition of this enzyme[51]. Later in the muscle, phosphocreatine is transformed into *creatinine* by spontaneous reaction, releasing it to the blood that transports it to the kidney where it is excreted in the urine.

Arginine is also required to remove urea through the urea cycle for detoxification of nitrogen compounds synthesized in the liver and has protective effect on oxidative stress in mice when this metabolite is supplemented in the diet[52]. *Urea* is the main compound of excretion of ammonia that is formed in the disintegration of amino acids and proteins, it is synthesized almost exclusively in the liver passing later to the blood to be rapidly excreted through the urine. As can be seen in Table 2, this metabolite increases in the kidney in mice fed DDE diet, but decrease when selenium is also added. *Ornithine* is an amino acid that plays an important role in the urea cycle as a carrier of $NH_4^+$, being one of the products in the formation of urea from L-arginine by the enzyme arginase. The flow of nitrogen through the urea cycle varies with the diet of an organism. In this study, an increase in the levels of ornithine (1.71-fold increase) and the correlative decrease in the levels of *aspartic acid* (0.45-fold decrease) and urea (0.48-fold decrease) in the liver of *Mus spretus* fed diet with DDE have been observed. These results suggest that aspartic acid formed in mitochondria by transamination between oxaloacetate and glutamate can be transported to the cytosol, where it acts as a nitrogen donor in the reaction of the urea cycle catalyzed by argininosuccinate synthetase, leading to an increase in the production of ornithine and urea. The latter will pass through the blood to the kidney where it is quickly excreted through the urine. This effect is attenuated when Se and DDE are added simultaneously to the diet, as shown by the fold-change values obtained for ornithine (1.55-fold increase), aspartic acid (0.61-fold decrease) and urea (0.66-fold decrease) these metabolites in this group (Tables 1 and 2).

### 3.3.2. Glycolysis and Kreb´s cycle

An increase in the levels of glucose and its derivative glucose-6-phosphate was observed (Table 2) in the *Mus spretus* mice fed DDE diet. This fact could be associated with hyperglycemia and alteration of glucose an lipid metabolism described in mice exposed to DDE[53–55]. These previous studies demonstrated the onset of a metabolic switch towards aerobic glycolysis as the only way to generate ATP in DDE exposed hepatic cells, where oxidative phosphorylation resulted impaired by mitochondria membrane oxidative damage. In these cells under the so-called Warburg effect[56,57], several enzymes, including the lactate dehydrogenase and the glutamine-pyruvate transaminase (GTP2), are deregulated and their activity enhanced. The generated lactate is quickly exported from the liver to the blood, where both local and distant tissues can take it up and use it as a fuel[58], and the lactic acid levels in the liver go down, as observed in the DDE exposed mice (Table 2).

Metabolic reprogramming is critical to oncogenesis[57]. The results observed in this work demonstrate the occurrence of these metabolic changes in *Mus spretus* exposed to DDE, thus providing information on the carcinogenic effects of said toxicant. In addition to

aerobic glycolytic activation, cancer cells frequently activate glutamine consumption as a carbon source for Krebs cycle anaplerosis in cancer cells[59]. In DDE exposed mice, we observed a reduction in the glutamine levels and also in those of L-aspartic acid, which can be converted by transamination to oxaloacetate and subsequently enter into the Krebs cycle[60]. These changes indicate an energy requirement by the organism due to the toxic that cell tries to counteract by providing intermediates to the Krebs cycle, partially inhibited by the deviation of pyruvate to the lactate synthesis pathway. Glutamine is the main source of $NH_4^+$ for the body and decreases also in response to cellular acidosis caused by DDE[61]. it is noteworthy the opposite effect of DDE over the glutamine and aspartic levels in the liver and the brain.

The incorporation of Se to the diet partially ameliorates the effect of DDE exposure on several metabolites, probably by its antioxidative properties that protect the integrity and functionality of mitochondria. However, the effect is only partial and did not completely prevent the metabolic shift caused by DDE exposure that leads to disturbed lipogenesis, hepatic steatosis and alterations in the synthesis of hormones and other cell signals, as previously reported[25] and discussed ahead.

The absence of glucose metabolism changes in the brain was not completely unexpected, since glucose metabolism is tightly regulated in this organ to avoid several diseases affecting both the brain itself as well as the entire organism caused by disturbed glucose metabolism[62].

As with other metabolites, it was remarkable the opposite effect of DDE over the glutamine and aspartic levels in the liver and the brain. Glutamine, the most common plasma amino acid, is taken up by brain cells to serve as a nitrogen donor for biosynthesis and as an important anaplerotic substrate in the Krebs cycle what might explain the increased levels of this amino acid in the brain of DDE exposed mice. We cannot rule out that increased glutamine results from an increased activity of glutamine synthetase in the astrocytes to capturing excess ammonia and glutamate protect neurons against excitotoxicity[63]. The increased levels of glutamine in the brain of DDE exposed mice might be the cause of neurological alterations attributed to this organochlorine[64]. As shown in Table 2, the presence of selenium as part of the diet of the DDE exposed mice avoided the glutamine increase in the brain, which could be achieved by glutamine conversion to glutamate to fuel the Krebs cycle. Glutamate can then be converted to aspartate, involved in the biosynthesis of purines and the urea cycle, explaining the elevated levels of this amino acid in the brain of DDE exposed mice. Selenium potentiated the DDE effect over the aspartic levels helping to remove ammonia through the urea cycle.

### 3.3.3. Lipid metabolism.

Alterations of cell membrane components have been observed in mice exposed to DDE and Se. These components include the decrease of two classes of phospholipids: (i) Those

that contain *choline* in their structure, such as lysophosphatidylcholines (LPCs) (degradation products of *phosphatidylcholines* PCs) and (ii) *lysophosphatidylethanolamines* (degradation products of phosphatidiethanolamines PEs). Both phospholipids are major components of plasma membranes, which are involved in pathological mechanisms and key cellular functions, such as signal transduction, apoptosis and necrosis[65,66]. The decrease in LPCs in *Mus spretus* liver after DDE addition (Table 1) was accompanied in parallel with an increase in *free fatty acid (FFA)* levels. These two classes of compounds are the components that form the LPCs, which confirms the rupture of the membrane by lipid peroxidation[67]. This process begins when phospholipase A2 releases FFA from PCs to produce LPCs, which are subsequently hydrolyzed to choline and degradation by-products such as *myoinositol-phosphate*, glycerol and *glycerol-3-phosphate* (Table2), a fact that is confirmed by the increase of the intensities of these last three metabolites. In this study, this cell membrane degradation effect is attenuated in the mice fed Se and DDE diet, as demonstrated by the Fold Change values obtained for these metabolites.

### 3.3.4. Fatty acid β-oxidation

The liver is the key organ in maintaining lipid homeostasis, being the main site of fatty acid oxidation together with the muscle (mainly β-oxidation, the process by which the fatty acids are broken down to generate acetyl-CoA that in the end generates energy to the cell in the form of ATP, takes place into the mitochondria) and it is the sole organ able to de novo synthesizes fatty acids by lipogenesis[47]. Disturbances in the levels of triglyceride can also be observed in response to the toxicity caused by DDE. Alterations in *triglyceride* levels have been previously demonstrated in mice exposed to DDE and its derivatives[53,68]. In the study, a decrease in the levels of hepatic triglycerides was observed, in agreement with previous results obtained for mice subject to exposure to DDE[53]. However, an increase in *diglycerides* was also observed, as well as an increase in fatty acids and cholesterol, suggesting a situation of hyperlipidemia, which is one of the most important factors of vascular risk. In fact, there are many studies that show the direct association that exists between exposure to DDE and hepatic steatosis (fatty liver) that leads to a lipid increase in the liver[53,69,70]. In the presence of Se this effect decreases, since the intensities corresponding to the hepatic lipids (diglycerides, fatty acids) are lower as shown by the fold-change values shown in Tables 1 and 2.

*Carnitines (CAR)* are essential in the transport of lipids from the cytosol to the mitochondria for the production of energy by β-oxidation, among these lipids we can find the fatty acids. The increase of the levels of fatty acids and the correlative increase of carnitines in *Mus spretus* liver fed diet with DDE and into a lesser extent with DDE and Se, explain this fact and could be related to a protective mechanism induced by lipid peroxidation (oxidative degradation of lipids) caused by the toxic compound (Table 1).

3.3.5. Nucleotide metabolism

Finally, alterations in nucleotide metabolism are observed with an increase in *adenylic acid* and a decrease in *inosine* after DDE addition. Under oxidative stress, nucleotides with purine bases, such as adenylic acid (AMP), are oxidatively degraded, transforming into the nucleoside inosine and finally passing to uric acid, which is excreted in the urine. In this way, an increase in adenylic acid could be considered as a marker of oxidative stress (via oxidative phosphorylation), but it can also have important consequences in the homeostasis of cellular energy, since it plays a central role in the metabolism of glucose and lipids through the enzymatic complex AMPK (protein kinase activated by AMP)[71]. In mice fed Se diet, the response of these two metabolites is less pronounced, thus demonstrating the protective effect exerted by Se on the toxicity of DDE (see fold change in table 1 and 2).

## 4. Conclusions

Taking into account the complexity of biological systems and the environment, some important effects may be caused by the interplay among two xenobiotics, but such interactions are rarely reported. This work shows for the first time the antagonism between DDE and Se in mammals using a metabolomic platform. DIMS is a very suitable technique for fast metabolomic evaluation of toxicological effects of chemical cocktails, such as DDE and Se, which can be complemented by GC-MS to extend the metabolic coverage. In addition, analysis of polar and nonpolar extracts using positive and negative mode allows characterizing a great number of possible biomarkers of DDE toxicity and the protective effect of selenium. Perturbation of cell membrane stability, energy cycle and methylation process has been observed. Therefore, this analytical methodology can contribute to the knowledge of chemical cocktails impact in mammals and its consequences.

## Acknowledgements

This work has been supported by the projects CTM2015-67902-C2-1-P and PG2018-096608-B-C21 from the Spanish Ministry of Economy and Competitiveness and P12-FQM-0442 and BIO-1657 from the Regional Ministry of Economy, Innovation, Science and Employment (Andalusian Government, Spain). Gema Rodríguez Moro thanks to Spanish Ministry of Economy and Competitiveness for a PhD scholarship (BES-2013-064501). Sara Ramírez Acosta thanks to Spanish Ministry of Economy and Competitiveness for a PhD scholarship (BES-2016-076364). Finally, authors are grateful to FEDER (European Community) for financial support, grants number UNHU13-1E-1611 and UNHU15-CE-3140.

## Compliance with ethical standards

## Conflict of interest

The authors declare that they have no conflict of interest.

## Ethical approval

All animals received humane care in compliance with the guidelines of animal care and use of the European Community and the experimental design was made seeking to minimize the number of animals and following the guidelines of the Bioethics Committee of the University of Córdoba (Spain).

**Supporting Information** [Supplementary material contains Spectra, score plots obtained by PLS, accession number of metabolites, Summary stats of metabolites, RDS in the quality control samples and p-values and pathway impact scores for the most significant pathways of each organ].

## 5. References


(1) García-Barrera, T.; Gómez-Ariza, J. L.; González-Fernández, M.; Moreno, F.; García-Sevillano, M. A.; Gómez-Jacinto, V. Biological Responses Related to Agonistic, Antagonistic and Synergistic Interactions of Chemical Species. *Anal. Bioanal. Chem.* **2012**, *403* (8), 2237–2253.

(2) Park, K.; Mozaffarian, D. Omega-3 Fatty Acids, Mercury, and Selenium in Fish and the Risk of Cardiovascular Diseases. *Curr. Atheroscler. Rep.* **2010**, *12* (6), 414–422.

(3) Choi, A. L.; Budtz-Jørgensen, E.; Jørgensen, P. J.; Steuerwald, U.; Debes, F.; Weihe, P.; Grandjean, P. Selenium as a Potential Protective Factor against Mercury Developmental Neurotoxicity. *Environ. Res.* **2008**, *107* (1), 45–52.

(4) Beyrouty, P.; Chan, H. M. Co-Consumption of Selenium and Vitamin E Altered the Reproductive and Developmental Toxicity of Methylmercury in Rats. *Neurotoxicol. Teratol.* **2006**, *28* (1), 49–58.

(5) Kolachi, N. F.; Kazi, T. G.; Wadhwa, S. K.; Afridi, H. I.; Baig, J. A.; Khan, S.; Shah, F. Evaluation of Selenium in Biological Sample of Arsenic Exposed Female Skin Lesions and Skin Cancer Patients with Related to Non-Exposed Skin Cancer Patients. *Sci. Total Environ.* **2011**, *409* (17), 3092–3097.

(6) Hurná, E.; Siklenka, P.; Hurná, S. Effect of Selenium on Cadmium Genotoxicity Investigated by Micronucleus Assay. *Vet. Med. (Praha).* **1997**, *42* (11), 339–342.

(7) Nehru, L. B.; Bansal, M. P. Effect of Selenium Supplementation on the Glutathione Redox System in the Kidney of Mice after Chronic Cadmium Exposures. *J. Appl. Toxicol.* **1997**, *17* (1), 81–84.

(8) El-Maraghy, S. A.; Gad, M. Z.; Fahim, A. T.; Hamdy, M. A. Effect of Cadmium and Aluminum Intake on the Antioxidant Status and Lipid Peroxidation in Rat Tissues. *J. Biochem. Mol. Toxicol.* **2001**, *15* (4), 207–214.

(9) Stadtman, T. C. Biosynthesis and Function of Selenocysteine-Containing Enzymes. *J. Biol. Chem.* **1991**, *266* (25), 16257–16260.

(10) Lai, I. K.; Chai, Y.; Simmons, D.; Watson, W. H.; Tan, R.; Haschek, W. M.; Wang, K.; Wang, B.; Ludewig, G.; Robertson, L. W. Dietary Selenium as a Modulator of PCB 126-Induced Hepatotoxicity in Male Sprague-Dawley Rats. *Toxicol. Sci.* **2011**, *124* (1), 202–214.

(11) Raines, A. M.; Sunde, R. A. Selenium Toxicity but Not Deficient or Super-Nutritional Selenium Status Vastly Alters the Transcriptome in Rodents. *BMC Genomics* **2011**, *12*:26-40.

(12) Chen, J.; Berry, M. J. Selenium and Selenoproteins in the Brain and Brain Diseases. *J. Neurochem.* **2004**, *86* (1), 1–12.

(13) Milošević, M. D.; Paunović, M. G.; Matić, M. M.; Ognjanović, B. I.; Saičić, Z. S. The Ameliorating Effects of Selenium and Vitamin C against Fenitrothion-Induced Blood Toxicity in Wistar Rats. *Environ. Toxicol. Pharmacol.* **2017**, *56*, 204–209.

(14) Suwondo, A.; Achmadi, U. F.; Suratman. The Effect of Selenium Supplementation on Hemoglobin among Farmers Working as Pesticide Sprayers. *Adv. Sci. Lett.* **2017**, *23* (4), 3361–3363.

(15) *Toxicological Profile: For DDT,DDD, and DDE*; Agency for toxic substance and disease registry, 2002.

(16) Longnecker, M. P.; Gladen, B. C.; Cupul-Uicab, L. A.; Romano-Riquer, S. P.; Weber, J.-P.; Chapin, R. E.; Hernández-Ávila, M. In Utero Exposure to the

Antiandrogen 1,1-Dichloro-2,2-Bis(p-Chlorophenyl) Ethylene (DDE) in Relation to Anogenital Distance in Male Newborns from Chiapas, México. *Am. J. Epidemiol.* **2007**, *165* (9), 1015–1022.

(17) Compta, Y.; Parkkinen, L.; O'Sullivan, S. S.; Vandrovcova, J.; Holton, J. L.; Collins, C.; Lashley, T.; Kallis, C.; Williams, D. R.; De Silva, R.; et al. Lewy- and Alzheimer-Type Pathologies in Parkinson's Disease Dementia: Which Is More Important? *Brain* **2011**, *134* (5), 1493–1505.

(18) Dowling, V.; Hoarau, P. C.; Romeo, M.; O'Halloran, J.; Van Pelt, F.; O'Brien, N.; Sheehan, D. Protein Carbonylation and Heat Shock Response in Ruditapes Decussatus Following P,p′-Dichlorodiphenyldichloroethylene (DDE) Exposure: A Proteomic Approach Reveals That DDE Causes Oxidative Stress. *Aquat. Toxicol.* **2006**, *77* (1), 11–18.

(19) *Regulatory Determinations Support Document for Selected Contaminants from the Second Drinking Water Contaminant Candidate List (CCL 2) EPA Report 815-R-08-012*; 2008.

(20) Mateo, R.; Millán, J.; Rodríguez-Estival, J.; Camarero, P. R.; Palomares, F.; Ortiz-Santaliestra, M. E. Levels of Organochlorine Pesticides and Polychlorinated Biphenyls in the Critically Endangered Iberian Lynx and Other Sympatric Carnivores in Spain. *Chemosphere* **2012**, *86* (7), 691–700.

(21) Ruiz-Laguna, J.; Abril, N.; García-Barrera, T.; Gómez-Ariza, J.-L.; López-Barea, J.; Pueyo, C. Absolute Transcript Expression Signatures of Cyp and Gst Genes in Mus Spretus to Detect Environmental Contamination. *Environ. Sci. Technol.* **2006**, *40* (11), 3646–3652.

(22) Montes-Nieto, R.; Fuentes-Almagro, C. A.; Bonilla-Valverde, D.; Prieto-Alamo, M.-J.; Jurado, J.; Carrascal, M.; Gómez-Ariza, J. L.; López-Barea, J.; Pueyo, C. Proteomics in Free-Living Mus Spretus to Monitor Terrestrial Ecosystems. *Proteomics* **2007**, *7* (23), 4376–4387.

(23) Romero-Ruiz, A.; Carrascal, M.; Alhama, J.; Gómez-Ariza, J. L.; Abian, J.; López-Barea, J. Utility of Proteomics to Assess Pollutant Response of Clams from the Doñana Bank of Guadalquivir Estuary (SW Spain). *Proteomics* **2006**, *6 Suppl 1*, S245-255.

(24) Bundy, J. G.; Davey, M. P.; Viant, M. R. Environmental Metabolomics: A Critical Review and Future Perspectives. *Metabolomics* **2009**, *5* (1), 3-21.

(25) Morales-Prieto, N.; Ruiz-Laguna, J.; Abril, N. Dietary Se Supplementation Partially Restores the REDOX Proteomic Map of M. Spretus Liver Exposed to P,p′-DDE. *Food Chem. Toxicol.* **2018**, *114*, 292–301.

(26) García-Barrera, T.; Rodríguez-Moro, G.; Callejón-Leblic, B.; Arias-Borrego, A.; Gómez-Ariza, J. L. Mass Spectrometry Based Analytical Approaches and Pitfalls for Toxicometabolomics of Arsenic in Mammals: A Tutorial Review. *Anal. Chim. Acta* **2018**, *1000*, 41–66.

(27) Dunn, W. B.; Erban, A.; Weber, R. J. M.; Creek, D. J.; Brown, M.; Breitling, R.; Hankemeier, T.; Goodacre, R.; Neumann, S.; Kopka, J.; et al. Mass Appeal: Metabolite Identification in Mass Spectrometry-Focused Untargeted Metabolomics. *Metabolomics* **2013**, *9* (SUPPL.1).

(28) García-Sevillano, M. A.; Contreras-Acuña, M.; García-Barrera, T.; Navarro, F.; Gómez-Ariza, J. L. Metabolomic Study in Plasma, Liver and Kidney of Mice Exposed to Inorganic Arsenic Based on Mass Spectrometry. *Anal. Bioanal. Chem.* **2014**, *406* (5), 1455–1469.

(29) García-Sevillano, M. A.; Abril, N.; Fernández-Cisnal, R.; García-Barrera, T.; Pueyo, C.; López-Barea, J.; Gómez-Ariza, J. L. Functional Genomics and

Metabolomics Reveal the Toxicological Effects of Cadmium in Mus Musculus Mice. *Metabolomics* **2015**, 11 (5), 1432-1450.

(30) Draper, J.; Lloyd, A. J.; Goodacre, R.; Beckmann, M. Flow Infusion Electrospray Ionisation Mass Spectrometry for High Throughput, Non-Targeted Metabolite Fingerprinting: A Review. *Metabolomics* **2013**, *9* (SUPPL.1), 4-29.

(31) González-Domínguez, R.; García-Barrera, T.; Gómez-Ariza, J. L. Using Direct Infusion Mass Spectrometry for Serum Metabolomics in Alzheimer's Disease. *Anal. Bioanal. Chem.* **2014**, *406* (28), 7137–7148.

(32) Viant, M. R.; Sommer, U. Mass Spectrometry Based Environmental Metabolomics: A Primer and Review. *Metabolomics* **2012**, *9* (S1), 144–158.

(33) Pasha, S. T. Changes in Hepatic Microsomal Enzymes due to DDT, DDE and DDD Feeding in CF-1 Mice. *Indian J. Med. Res.* **1981**, *74* (6), 926–930.

(34) Galassi, S.; Bettinetti, R.; Neri, M. C.; Falandysz, J.; Kotecka, W.; King, I.; Lo, S.; Klingmueller, D.; Schulte-Oehlmann, U. pp′DDE Contamination of the Blood and Diet in Central European Populations. *Sci. Total Environ.* **2008**, *390* (1), 45–52.

(35) Begley, P.; Francis-McIntyre, S.; Dunn, W. B.; Broadhurst, D. I.; Halsall, A.; Tseng, A.; Knowles, J.; Goodacre, R.; Kell, D. B. Development and Performance of a Gas Chromatography-Time-of-Flight Mass Spectrometry Analysis for Large-Scale Nontargeted Metabolomic Studies of Human Serum. *Anal. Chem.* **2009**, *81* (16), 7038-7046.

(36) Katajamaa, M.; Oresic, M. Data Processing for Mass Spectrometry-Based Metabolomics. *J. Chromatogr. A* **2007**, *1158* (1–2), 318–328.

(37) Smith, C. A.; Want, E. J.; O'Maille, G.; Abagyan, R.; Siuzdak, G. XCMS: Processing Mass Spectrometry Data for Metabolite Profiling Using Nonlinear Peak Alignment, Matching, and Identification. *Anal. Chem.* **2006**, *78* (3), 779–787.

(38) Veselkov, K. A.; Vingara, L. K.; Masson, P.; Robinette, S. L.; Want, E.; Li, J. V; Barton, R. H.; Boursier-Neyret, C.; Walther, B.; Ebbels, T. M.; et al. Optimized Preprocessing of Ultra-Performance Liquid Chromatography/mass Spectrometry Urinary Metabolic Profiles for Improved Information Recovery. *Anal. Chem.* **2011**, *83* (15), 5864–5872.

(39) Sumner, L. W.; Amberg, A.; Barrett, D.; Beale, M. H.; Beger, R.; Daykin, C. A.; Fan, T. W.-M.; Fiehn, O.; Goodacre, R.; Griffin, J. L.; et al. Proposed Minimum Reporting Standards for Chemical Analysis: Chemical Analysis Working Group (CAWG) Metabolomics Standards Initiative (MSI). *Metabolomics* **2007**, *3* (3), 211–221.

(40) Schymanski, E. L.; Jeon, J.; Gulde, R.; Fenner, K.; Ruff, M.; Singer, H. P.; Hollender, J. Identifying Small Molecules via High Resolution Mass Spectrometry: Communicating Confidence. *Environ. Sci. Technol.* **2014**, *48* (4), 2097–2098.

(41) van den Berg, R. A.; Hoefsloot, H. C. J.; Westerhuis, J. A.; Smilde, A. K.; van der Werf, M. J. Centering, Scaling, and Transformations: Improving the Biological Information Content of Metabolomics Data. *BMC Genomics* **2006**, *7*, *142*.

(42) González-Dominguez, R.; García-Barrera, T.; Gõmez-Ariza, J.-L. Iberian Ham Typification by Direct Infusion Electrospray and Photospray Ionization Mass Spectrometry Fingerprinting. *Rapid Commun. Mass Spectrom.* **2012**, *26* (7), 835–844.

(43) Vernez, L.; Hopfgartner, G.; Wenk, M.; Krähenbühl, S. Determination of Carnitine and Acylcarnitines in Urine by High-Performance Liquid Chromatography-Electrospray Ionization Ion Trap Tandem Mass Spectrometry. *J. Chromatogr. A* **2003**, *984* (2), 203–213.

(44) García-Sevillano, M. A.; García-Barrera, T.; Navarro, F.; Gailer, J.; Gómez-Ariza, J. L. Use of Elemental and Molecular-Mass Spectrometry to Assess the Toxicological Effects of Inorganic Mercury in the Mouse Mus Musculus. *Anal. Bioanal. Chem.* **2014**, *406* (24), 5853–5865.
(45) García-Sevillano, M. T.; García-Barrera, T.; Navarro-Roldán, F.; Montero-Lobato, Z.; Gómez-Ariza, J. L. A Combination of Metallomics and Metabolomics Studies to Evaluate the Effects of Metal Interactions in Mammals. Application to Mus Musculus Mice under Arsenic/cadmium Exposure. *J. Proteomics* **2014**, *104*, *66-79*.
(46) Degli Esposti, D.; Hamelin, J.; Bosselut, N.; Saffroy, R.; Sebagh, M.; Pommier, A.; Martel, C.; Lemoine, A. Mitochondrial Roles and Cytoprotection in Chronic Liver Injury. *Biochem. Res. Int.* **2012,** 387626.
(47) Fabbrini, E.; Sullivan, S.; Klein, S. Obesity and Nonalcoholic Fatty Liver Disease: Biochemical, Metabolic, and Clinical Implications. *Hepatology* **2010**, *51* (2), 679–689.
(48) Liang, X.; Zhang, L.; Natarajan, S. K.; Becker, D. . Proline Mechanisms of Stress Survival. *Antioxidants Redox Signal.* **2013**, *19* (9), 998–1011.
(49) Suzuki, K. T.; Doi, C.; Suzuki, N. Metabolism of 76Se-Methylselenocysteine Compared with that of 77Se-Selenomethionine and 82Se-Selenite. **2006**, *217* (2), 185–195.
(50) Donohue, J.M., Abernathy, C.O. Exposure to Inorganic Arsenic from Fish and Shellfish. In *Arsenic Exposure and Health Effects III*; Chappell, W.R., Abernathy, C.O., Calderon, R. L., Ed.; Amsterdam, 1999; pp 89–98.
(51) García-Sevillano, M. Á.; García-Barrera, T.; Abril, N.; Pueyo, C.; López-Barea, J.; Gómez-Ariza, J. L. Omics Technologies and Their Applications to Evaluate Metal Toxicity in Mice M. Spretus as a Bioindicator. *J. Proteomics* **2014**, *104*, 4–23.
(52) Dasgupta, T.; Hebbel, R. P.; Kaul, D. K. Protective Effect of Arginine on Oxidative Stress in Transgenic Sickle Mouse Models. *Free Radic. Biol. Med.* **2006**, *41* (12), 1771-1780.
(53) Howell, G. E.; Mulligan, C.; Meek, E.; Chambers, J. E. Effect of Chronic P,p'-dichlorodiphenyldichloroethylene (DDE) Exposure on High Fat Diet-Induced Alterations in Glucose and Lipid Metabolism in Male C57BL/6H Mice. *Toxicology* **2015**, *328*, 112–122.
(54) Howell, G. E.; Meek, E.; Kilic, J.; Mohns, M.; Mulligan, C.; Chambers, J. E. Exposure to P,p'-dichlorodiphenyldichloroethylene (DDE) Induces Fasting Hyperglycemia without Insulin Resistance in Male C57BL/6H Mice. *Toxicology* **2014**, *320*, 6–14.
(55) Morales-Prieto, N.; Abril, N. REDOX Proteomics Reveals Energy Metabolism Alterations in the Liver of M. Spretus Mice Exposed to P, P′-DDE. *Chemosphere* **2017**, *186*, 848–863.
(56) Tong, W.-H.; Sourbier, C.; Kovtunovych, G.; Jeong, S. Y.; Vira, M.; Ghosh, M.; Romero, V. V.; Sougrat, R.; Vaulont, S.; Viollet, B.; et al. The Glycolytic Shift in Fumarate-Hydratase-Deficient Kidney Cancer Lowers AMPK Levels, Increases Anabolic Propensities and Lowers Cellular Iron Levels. *Cancer Cell* **2011**, *20* (3), 315–327.
(57) Desideri, E.; Vegliante, R.; Ciriolo, M. R. Mitochondrial Dysfunctions in Cancer: Genetic Defects and Oncogenic Signaling Impinging on TCA Cycle Activity. *Cancer Lett.* **2015**, *356* (2), 217–223.
(58) Goodwin, M. L.; B, Gladden, L.; Nijsten, M. W. N.; Jones, K. B. Lactate and

Cancer: Revisiting the Warburg Effect in an Era of Lactate Shuttling. In *Frontiers in Nutrition*; 2014.

(59) Smith, B.; Schafer, X. L.; Ambeskovic, A.; Spencer, C. M.; Land, H.; Munger, J. Addiction to Coupling of the Warburg Effect with Glutamine Catabolism in Cancer Cells. *Cell Rep.* **2016**, *17* (3), 821–836.

(60) Nomme, J.; Su, Y.; Lavie, A. Elucidation of the Specific Function of the Conserved Threonine Triad Responsible for Human L-Asparaginase Autocleavage and Substrate Hydrolysis. *J. Mol. Biol.* **2014**, *426* (13), 2471–2485.

(61) Hems, D. A. Metabolism of Glutamine and Glutamic Acid by Isolated Perfused Kidneys of Normal and Acidotic Rats. *Biochem. J.* **1972**, *130* (3), 671–680.

(62) Mergenthaler, P.; Lindauer, U.; Dienel, G. A.; Meisel, A. Sugar for the Brain: The Role of Glucose in Physiological and Pathological Brain Function. *Trends Neurosci.* **2013**, *36* (10), 587–597.

(63) Suárez, I.; Bodega, G.; Fernández, B. Glutamine Synthetase in Brain: Effect of Ammonia. *Neurochem. Int.* **2002**, *41* (2–3), 123–142.

(64) Wnuk, A.; Rzemieniec, J.; Litwa, E.; Lasoń, W.; Krzeptowski, W.; Wójtowicz, A. K.; Kajta, M. The Crucial Involvement of Retinoid X Receptors in DDE Neurotoxicity. *Neurotox. Res.* **2016**, *29* (1), 155–172.

(65) Koivusalo, M.; Haimi, P.; Heikinheimo, L.; Kostiainen, R.; Somerharju, P. Quantitative Determination of Phospholipid Compositions by Esi-Ms: Effects of Acyl Chain Length, Unsaturation, and Lipid Concentration on Instrument Response. *J. Lipid Res.* **2001**, *42* (4), 663–672.

(66) Bashir, S.; Sharma, Y.; Irshad, M.; Gupta, S. D.; Dogra, T. D. Arsenic-Induced Cell Death in Liver and Brain of Experimental Rats. *Basic Clin. Pharmacol. Toxicol.* **2006**, *98* (1), 38–43.

(67) Griffin, J. .; Mann, C. .; Scott, J.; Shoulders, C. .; Nicholson, J. . Choline Containing Metabolites during Cell Transfection: An Insight into Magnetic Resonance Spectroscopy Detectable Changes. *FEBS Lett.* **2001**, *509* (2), 263–266.

(68) La Merrill, M.; Karey, E.; Moshier, E.; Lindtner, C.; La Frano, M. R.; Newman, J. W.; Buettner, C. Perinatal Exposure of Mice to the Pesticide DDT Impairs Energy Expenditure and Metabolism in Adult Female Offspring. *PLoS One* **2014**, *9* (7), e103337.

(69) Ibrahim, M. M.; Fjære, E.; Lock, E.-J.; Naville, D.; Amlund, H.; Meugnier, E.; Battistoni, B. L. M.; Frøyland, L.; Madsen, L.; Jessen, N.; et al. Chronic Consumption of Farmed Salmon Containing Persistent Organic Pollutants Causes Insulin Resistance and Obesity in Mice. *PLoS One* **2011**, *6* (9), e25170.

(70) Ruzzin, J.; Petersen, R.; Meugnier, E.; Madsen, L.; Lock, E.-J.; Lillefosse, H.; Ma, T.; Pesenti, S.; Sonne, S. B.; Marstrand, T. T.; et al. Persistent Organic Pollutant Exposure Leads to Insulin Resistance Syndrome. *Environ. Health Perspect.* **2010**, *118* (4), 465–471.

(71) Nuevo Ordoñez, Y.; Montes-Bayón, M.; Blanco-González, E.; Sanz-Medel, A. Quantitative Analysis and Simultaneous Activity Measurements of Cu, Zn-Superoxide Dismutase in Red Blood Cells by HPLC-ICPMS. *Anal. Chem.* **2010**, *82* (6), 2387-2394.

## Tables

**Table 1.** Metabolites altered in liver, kidney and brain of *Mus spretus* mice fed DDE with and without selenium diet obtained by DI-ESI(+)-QTOF-MS

| Metabolites | m/z | Organ | Extract | Mice exposed to DDE | | | Mice exposed to DDE/Se | | | Mice exposed to Se | | |
|---|---|---|---|---|---|---|---|---|---|---|---|---|
| | | | | Response[a] | Fold change[b] | *p* value[c] | Response[a] | Fold change[b] | *p* value[c] | Response[a] | Fold change[b] | *p* value[c] |
| Urea | 61.041 ($H^+$) | Liver | Polar/ Nonpolar | ↓ | 0.48 | 0.025 | ↓ | 0.66 | 0.035 | ↓ | 0.61 | 0.025 |
| Pyruvate | 89.067 ($H^+$) | Kidney | Polar | ↓ | 0.54 | 0.041 | ↓ | 0.83 | 0.034 | ↓ | 0.37 | 0.013 |
| Choline | 104.109 ($H^+$) | Liver | Polar/ Nonpolar | ↓ | 0.47 | 0.011 | ↓ | 0.62 | 0.029 | ↓ | 0.76 | 0.023 |
| | | Brain | Polar/ Nonpolar | ↑ | 2.31 | 0.023 | NS | NS | NS | NS | NS | NS |
| Creatinina | 114.066 ($H^+$) | Liver | Polar | ↓ | 0.67 | 0.047 | ↓ | 0.73 | 0.041 | ↓ | 0.72 | 0.034 |
| Proline | 116.072($H^+$) | Kidney | Polar | ↑ | 2.69 | 0.028 | ↑ | 1.15 | 0.024 | NS | NS | NS |
| | | Brain | Polar | ↑ | 2.11 | 0.019 | ↑ | 2.06 | 0.023 | ↑ | 1.41 | 0.047 |
| Betaine | 118.091 ($H^+$) | Kidney | Polar | ↑ | 1.26 | 0.017 | ↓ | 0.78 | 0.036 | ↓ | 0.54 | 0.048 |
| | | Brain | Polar | ↑ | 1.73 | 0.032 | ↑ | 1.56 | 0.012 | ↑ | 1.31 | 0.031 |
| Cysteine | 122.038 ($H^+$) | Brain | Polar | ↑ | 1.75 | 0.025 | ↑ | 1.8 | 0.007 | NS | NS | NS |
| Hypoxanthine | 137.041 ($H^+$) | Brain | Polar | ↑ | 1.62 | 0.037 | ↑ | 1.48 | 0.031 | ↑ | 2.63 | 0.006 |
| PE | 142.162 ($H^+$) | Kidney | Polar | ↓ | 0.63 | 0.021 | ↓ | 0.75 | 0.019 | ↓ | 0.59 | 0.023 |
| Glutamate | 148.047 ($H^+$) | Brain | Nonpolar | ↑ | 1.15 | 0.048 | ↓ | 0.49 | 0.014 | NS | NS | NS |
| Methionine | 150.041 ($H^+$) | Brain | Polar | ↑ | 1.61 | 0.041 | ↑ | 1.64 | 0.046 | ↑ | 1.41 | 0.027 |
| Xanthine | 151.023 ($-H^+$) | Brain | Polar | ↑ | 2.09 | 0.006 | ↑ | 2.04 | 0.034 | ↑ | 2.65 | 0.018 |
| Hippuric acid | 178.041 ($-H^+$) | Kidney | Polar | ↑ | 2.39 | 0.019 | ↑ | 2.42 | 0.026 | ↑ | 1.75 | 0.014 |

| | | | | | | | | | | | | |
|---|---|---|---|---|---|---|---|---|---|---|---|---|
| Phosphocholine | 184.069 ($H^+$) | Brain | Polar | ↑ | 2.25 | 0.024 | ↑ | 1.53 | 0.01 | NS | NS | NS |
| (Iso-)citrate | 191.015 ($-H^+$) | Kidney | Polar | ↑ | 0.37 | 0.009 | ↓ | 0.52 | 0.021 | ↓ | 0.43 | 0.041 |
| | | Brain | Polar | NS | NS | NS | ↑ | 1.16 | 0.037 | ↑ | 1.62 | 0.023 |
| C2-CAR | 204.126 ($H^+$) | Brain | Polar | ↓ | 0.13 | 0.044 | ↓ | 0.95 | 0.045 | ↓ | 0.38 | 0.029 |
| C4-CAR | 232.139 ($H^+$) | Brain | Polar | ↓ | 0.6 | 0.041 | NS | NS | NS | ↓ | 0.54 | 0.035 |
| C5-CAR | 246.176 ($H^+$) | Kidney | Polar | ↑ | 1.7 | 0.039 | NS | NS | NS | ↑ | 1.87 | 0.015 |
| Palmitoleic acid | 253.212 ($-H^+$) | Kidney | Polar | ↑ | 1.99 | 0.042 | ↑ | 1.62 | 0.024 | ↑ | 2.22 | 0.021 |
| GPC | 258.094 ($H^+$) | Brain | Nonpolar | ↓ | 0.57 | 0.035 | ↓ | 0.48 | 0.019 | ↓ | 0.83 | 0.037 |
| C6-CAR | 260.158 ($H^+$) | Kidney | Polar | ↑ | 1.63 | 0.036 | NS | NS | NS | ↑ | 2.34 | 0.014 |
| Inosine | 269.108 ($H^+$) | Liver | Polar | ↓ | 0.39 | 0.027 | ↓ | 0.69 | 0.046 | ↓ | 0.45 | 0.031 |
| | | Kidney | Polar | ↓ | 0.61 | 0.034 | ↓ | 0.84 | 0.036 | ↑ | 1.22 | 0.042 |
| Linoleic acid | 279.233 ($-H^+$) | Brain | Polar | ↑ | 1.76 | 0.012 | ↑ | 1.35 | 0.038 | ↑ | 1.59 | 0.035 |
| Oleic acid | 281.240 ($-H^+$) | Kidney | Polar | ↑ | 1.85 | 0.001 | ↑ | 2.05 | 0.04 | ↑ | 2.3 | 0.015 |
| | | Brain | Polar | ↑ | 1.98 | 0.021 | ↑ | 1.18 | 0.043 | ↑ | 1.65 | 0.019 |
| C18:1-CAR | 426.326 ($H^+$) | Liver | Polar | ↑ | 1.77 | 0.041 | ↑ | 1.66 | 0.019 | ↑ | 1.81 | 0.035 |
| | | Brain | Polar | ↓ | 0.56 | 0.038 | NS | NS | NS | NS | NS | NS |
| LPC(18:1) | 522.356 ($H^+$) | Liver | Polar/ Nonpolar | ↓ | 0.47 | 0.027 | ↑ | 0.78 | 0.029 | ↑ | 0.72 | 0.034 |
| LPE(22:2) | 534.340 ($H^+$) | Liver | Polar/ Nonpolar | ↓ | 0.75 | 0.031 | ↓ | 0.84 | 0.038 | ↓ | 0.56 | 0.046 |
| LPC(18:4) | 538.291 ($Na^+$) | Liver | Polar/ Nonpolar | ↓ | 0.58 | 0.021 | ↓ | 0.88 | 0.035 | ↓ | 0.79 | 0.028 |
| DAG (16:0/18:2) | 610.553 ($NH_4^+$) | Liver | Nonpolar | ↑ | 1.94 | 0.025 | ↑ | 1.51 | 0.046 | ↑ | 1.43 | 0.031 |
| DAG (16:0/18:1) | 612.567 ($NH_4^+$) | Liver | Nonpolar | ↑ | 1.89 | 0.043 | ↑ | 1.47 | 0.037 | ↑ | 1.79 | 0.02 |

| | | | | | | | | | | | | |
|---|---|---|---|---|---|---|---|---|---|---|---|---|
| DAG (18:3/18:1) | 634.567 ($NH4^+$) | Kidney | Nonpolar | ↓ | 0.62 | 0.022 | ↑ | 1.44 | 0.026 | ↑ | 2.28 | 0.016 |
| DAG (18:2/18:1) | 636.585 ($NH4^+$) | Kidney | Nonpolar | ↓ | 0.58 | 0.031 | ↑ | 1.61 | 0.021 | ↑ | 2.7 | 0.023 |
| | | Liver | Nonpolar | ↑ | 2.06 | 0.009 | ↑ | 1.38 | 0.045 | ↑ | 1.65 | 0.014 |
| PC (16:0/16:0) | 756.532 ($Na^+$) | Brain | Polar | ↑ | 1.66 | 0.017 | NS | NS | NS | NS | NS | NS |
| TAG(18:4/18:4/20:4) | 912.773 ($NH_4^+$) | Liver | Nonpolar | ↓ | 0.53 | 0.021 | ↓ | 0.64 | 0.032 | ↓ | 0.78 | 0.043 |
| | | Kidney | Nonpolar | ↑ | 1.14 | 0.034 | ↑ | 1.11 | 0.046 | ↑ | 2.07 | 0.021 |
| TAG (16:0/18:2/22:0) | 930.859 ($NH4^+$) | Kidney | Nonpolar | ↑ | 1.4 | 0.046 | ↑ | 1.1 | 0.038 | ↑ | 3.26 | 0.011 |
| TAG (16:0/18:1/22:0) | 932.859 ($NH4^+$) | Kidney | Nonpolar | ↑ | 1.39 | 0.028 | ↑ | 1.17 | 0.032 | ↑ | 3.92 | 0.02 |
| | | Liver | Nonpolar | ↓ | 0.75 | 0.039 | ↓ | 0.65 | 0.043 | ↓ | 0.71 | 0.031 |
| TAG (18:4/18:4/22:6) | 936.822 ($NH4^+$) | Kidney | Nonpolar | ↑ | 1.44 | 0.042 | ↑ | 1.15 | 0.047 | ↑ | 3.46 | 0.017 |
| | | Liver | Nonpolar | ↓ | 0.37 | 0.037 | ↓ | 0.56 | 0.038 | ↓ | 0.65 | 0.022 |
| TAG(18:3/18:4/22:6) | 938.777 ($NH_4^+$) | Liver | Nonpolar | ↓ | 0.59 | 0.023 | ↓ | 0.71 | 0.024 | ↓ | 0.63 | 0.031 |
| TAG (18:1/18:4/22:6) | 942.761 ($NH_4^+$) | Liver | Nonpolar | ↓ | 0.47 | 0.041 | ↓ | 0.77 | 0.039 | ↓ | 0.54 | 0.043 |

*CAR, carnitine; DG, diacilglicerol; GPC, glycerophosphocholine; LPC, lysophosphocoline; LPE, lisophosphoethanolamine; TAG, triacylglycerol; PE, phosphoethanolamine; PC, phosphocholine; NS: Not significative*

[a]Response: Variations observed for the groups exposed to DDE, Se and DDE with selenium against the control group: ↑ increase of the *m/z* signal, ↓ decrease of the *m/z* signal.

[b]Fold change: relation between the intensity of a metabolite in mice fed DDE and DDE with Se diet, against the control group.

[c]*p-value* corrected by Tukey test.

**Table 2:** Metabolites altered in liver, kidney and brain of *Mus spretus* mice fed DDE with and without selenium diet obtained by GC-MS.

| Metabolites | Retention Index | Organ | Mice exposed to DDE | | | Mice exposed to DDE and Se | | | Mice exposed to Se | | |
|---|---|---|---|---|---|---|---|---|---|---|---|
| | | | Response[a] | Fold-Change[b] | *p* value[C] | Response[a] | Fold-Change[b] | *p* value[c] | Response[a] | Fold-Change[b] | *p* value[c] |
| **Lactic acid** | **1054** | Liver | ↓ | 0.53 | 0.023 | ↓ | 0.63 | 0.036 | NS | NS | NS |
| **Valine** | **1210** | Kidney | ↑ | 2.64 | 0.012 | ↑ | 1.66 | 0.021 | ↑ | 2.91 | 0.016 |
| | | Brain | NS | NS | NS | ↑ | 2.3 | 0.011 | NS | NS | NS |
| **Urea** | **1252** | Kidney | ↑ | 1.62 | 0.034 | ↓ | 0.39 | 0.027 | NS | NS | NS |
| **Phosphoric acid** | **1267** | Kidney | ↑ | 2.36 | 0.023 | ↓ | 0.48 | 0.033 | ↓ | 0.47 | 0.043 |
| | | Brain | NS | NS | NS | ↓ | 0.27 | 0.037 | ↓ | 0.74 | 0.035 |
| **Glycerol** | **1279** | Kidney | ↑ | 2.62 | 0.011 | ↑ | 2.63 | 0.019 | NS | NS | NS |
| | | Liver | ↑ | 1.97 | 0.021 | ↑ | 1.65 | 0.023 | ↑ | 1.54 | 0.038 |
| **Glycine** | **1317** | Kidney | ↑ | 3.36 | 0.007 | ↑ | 2.92 | 0.009 | ↑ | 3.34 | 0.004 |
| | | Brain | ↑ | 1.64 | 0.019 | ↑ | 5.15 | 0.008 | ↑ | 2.78 | 0.015 |
| **Serine** | **1367** | Kidney | ↑ | 2 | 0.013 | ↑ | 1.87 | 0.036 | ↑ | 2.51 | 0.011 |
| | | Brain | NS | NS | NS | ↑ | 3.33 | 0.013 | ↑ | 2.26 | 0.023 |
| **Malic acid** | **1394** | Brain | ↑ | 2.26 | 0.016 | ↑ | 1.55 | 0.026 | ↑ | 1.98 | 0.042 |
| | | Kidney | ↑ | 1.83 | 0.031 | NS | NS | NS | NS | NS | NS |
| **Proline** | **1411** | Brain | ↑ | 1.81 | 0.035 | ↑ | 3.28 | 0.029 | ↑ | 1.71 | 0.031 |
| | | Kidney | ↑ | 2.49 | 0.016 | ↑ | 2.71 | 0.017 | ↑ | 2.67 | 0.016 |
| **Aspartic acid** | **1482** | Liver | ↓ | 0.45 | 0.038 | ↓ | 0.61 | 0.031 | ↓ | 0.64 | 0.037 |
| | | Brain | ↑ | 2.08 | 0.029 | ↑ | 3.24 | 0.016 | ↑ | 2.17 | 0.026 |
| | | Kidney | ↑ | 2.63 | 0.014 | ↑ | 1.92 | 0.034 | ↑ | 2.05 | 0.025 |
| **Purine** | **1550** | Kidney | ↑ | 2.2 | 0.031 | NS | NS | NS | ↑ | 2.79 | 0.019 |
| **Ornithine** | **1655** | Liver | ↑ | 1.71 | 0.046 | ↑ | 1.55 | 0.041 | ↑ | 1.45 | 0.029 |
| | | Kidney | ↓ | 0.47 | 0.037 | NS | NS | NS | ↓ | 0.34 | 0.017 |
| **Cysteine** | **1710** | Kidney | ↓ | 0.6 | 0.037 | NS | NS | NS | NS | NS | NS |

| | | | | | | | | | | | |
|---|---|---|---|---|---|---|---|---|---|---|---|
| **Glycerol-3-phosphate** | **1754** | Liver | ↑ | 1.82 | 0.019 | ↑ | 1.56 | 0.043 | ↑ | 1.75 | 0.035 |
| **Glutamine** | **1786** | Liver | ↓ | 0.43 | 0.022 | ↓ | 0.64 | 0.034 | ↓ | 0.78 | 0.029 |
| | | Kidney | ↑ | 2.92 | 0.023 | ↓ | 0.19 | 0.029 | ↑ | 2.32 | 0.009 |
| | | Brain | ↑ | 1.29 | 0.043 | ↓ | 0.24 | 0.018 | ↓ | 0.37 | 0.023 |
| **Fructose** | **1860** | Kidney | ↑ | 3.48 | 0.001 | ↑ | 3.36 | 0.014 | ↑ | 2.87 | 0.022 |
| **Galactose** | **1875** | Liver | ↑ | 1.67 | 0.031 | ↑ | 1.42 | 0.045 | ↑ | 1.75 | 0.022 |
| | | Brain | NS | NS | NS | ↑ | 1.77 | 0.034 | ↑ | 1.38 | 0.028 |
| | | Kidney | NS | NS | NS | ↑ | 2.63 | 0.041 | NS | NS | NS |
| **Glucose** | **1880** | Liver | ↑ | 1.96 | 0.042 | ↑ | 1.42 | 0.034 | ↑ | 1.67 | 0.037 |
| | | Kidney | ↑ | 2.64 | 0.016 | ↑ | 3.6 | 0.022 | ↑ | 3.03 | 0.011 |
| **Gluconic acid** | **1987** | Liver | ↑ | 1.69 | 0.015 | ↑ | 1.33 | 0.048 | ↑ | 1.32 | 0.043 |
| | | Kidney | ↓ | 0.38 | 0.036 | NS | NS | NS | ↑ | 2.68 | 0.005 |
| **Palmitic acid** | **2051** | Liver | ↑ | 2.27 | 0.022 | ↑ | 2.04 | 0.026 | ↑ | 1.98 | 0.019 |
| | | Kidney | ↑ | 2.46 | 0.029 | ↑ | 3.75 | 0.007 | ↑ | 2.16 | 0.015 |
| | | Brain | ↑ | 2.31 | 0.035 | ↑ | 2.28 | 0.011 | ↑ | 1.52 | 0.022 |
| **Inositol** | **2083** | Kidney | ↑ | 1.76 | 0.019 | ↑ | 2.88 | 0.005 | ↑ | 1.73 | 0.027 |
| | | Brain | ↑ | 3 | 0.009 | ↑ | 4.01 | 0.014 | ↑ | 2.17 | 0.024 |
| **Uric acid** | **2119** | Kidney | ↓ | 0.56 | 0.046 | NS | NS | NS | NS | NS | NS |
| **Linoleic acid** | **2135** | Liver | ↑ | 1.63 | 0.038 | ↑ | 1.44 | 0.037 | ↑ | 1.57 | 0.033 |
| | | Kidney | ↑ | 3.03 | 0.017 | ↑ | 2.77 | 0.023 | NS | NS | NS |
| **Oleic acid** | **2145** | Liver | ↑ | 2.17 | 0.026 | ↑ | 1.67 | 0.017 | ↑ | 1.52 | 0.032 |
| | | Kidney | NS | NS | NS | ↑ | 3.2 | 0.011 | NS | NS | NS |
| | | Brain | ↑ | 2.59 | 0.013 | ↑ | 1.89 | 0.015 | ↑ | 11.28 | 0.001 |
| **Stearic acid** | **2174** | Liver | ↑ | 1.54 | 0.023 | ↑ | 1.85 | 0.031 | ↑ | 1.59 | 0.015 |
| | | Kidney | ↑ | 1.56 | 0.036 | ↑ | 1.93 | 0.026 | ↑ | 1.76 | 0.021 |
| | | Brain | ↑ | 2.9 | 0.007 | ↑ | 2.86 | 0.007 | ↑ | 1.55 | 0.041 |

| | | | | | | | | | | | |
|---|---|---|---|---|---|---|---|---|---|---|---|
| **Glucose-6-phosphate** | **2287** | Liver | ↑ | 1.85 | 0.033 | ↑ | 1.63 | 0.046 | ↑ | 1.99 | 0.036 |

*NS: Not significative*

[a]Response: Variations observed for the groups exposed to DDE, Se and DDE with selenium against the control group: ↑ increase of the *m/z* signal, ↓ decrease of the *m/z* signal.
[b]Fold change: relation between the intensity of a metabolite in mice fed DDE and DDE with Se diet, against the control group.
[c]*p value* corrected by Tukey test.